

Ab Initio Structure Determination of Ammonium Hydrogen Alkyl Phosphates from X-ray Powder Diffraction Data

ANTONIA NEELS,^a HELEN STOECKLI-EVANS,^{a*} JOCHEN NEELS,^b ABRAHAM CLEARFIELD^c AND DAMODARA POOJARY^c

^aInstitut de Chimie, Université de Neuchâtel, Avenue de Bellevaux 51, CH-2000 Neuchâtel, Switzerland, ^bInstitut für Angewandte Chemie Berlin-Adlershof eV, Rudower Chaussee 5, D-12484 Berlin, Germany, and ^cDepartment of Chemistry, Texas A & M University, College Station, TX 77843, USA. E-mail: helen.stoeckli-evans@ich.unine.ch

(Received 6 August 1997; accepted 6 November 1997)

Abstract

The structures of three ammonium hydrogen alkyl phosphates, $\text{NH}_4\text{PO}_2(\text{OH})(\text{OR})$ [$R = \text{Me}$ (1), Et (2), Pr^i (3)], have been solved *ab initio* from X-ray powder diffraction data. The structure determinations were based on Patterson search methods combined with difference-Fourier techniques and the refinement was carried out using Rietveld methods. Powder diffraction data were first collected for all three compounds in the reflection mode using $\text{Cu } K_{\alpha 1+\alpha 2}$ radiation. A pronounced preferred orientation effect was found for all the samples, even by side-loading into a flat sample holder. A random orientation of the powder particles was obtained for (1) using a special suspension chamber for the sample preparation, while for (2) and (3) data were remeasured in capillaries using the transmission mode. Crystals of the ammonium hydrogen methyl phosphate (1) and the ammonium hydrogen ethyl phosphate (2) both belong to the monoclinic space group $P2_1/c$, $Z = 4$, with $a = 9.9645$ (4), $b = 7.1801$ (3), $c = 7.8897$ (3) Å and $\beta = 96.243$ (3)° for (1), and $a = 12.6453$ (4), $b = 7.1502$ (2), $c = 7.9738$ (2) Å and $\beta = 108.875$ (2)° for (2). The ammonium hydrogen isopropyl phosphate (3) crystallizes in space group An , $Z = 4$, with $a = 6.2475$ (2), $b = 29.3825$ (6), $c = 4.6305$ (1) Å and $\beta = 100.904$ (2)°. All three compounds are characterized by an extended hydrogen-bonding network involving the hydrogen phosphate units and the ammonium ions, forming double layers. The methyl (1), ethyl (2) and isopropyl groups (3), which point into the interlayer space, connect the layers by van der Waals interactions.

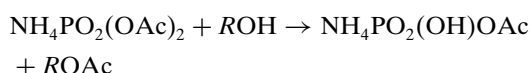
1. Introduction

The structures of several ammonium hydrogen alkyl phosphates have been determined in order to make a contribution to the study of compounds with extensive hydrogen-bonding networks. In the 1970s the structures of $(\text{NH}_4)_2\text{PO}_3(\text{OMe}) \cdot 2\text{H}_2\text{O}$ (Garbassi *et al.*, 1972) and $\text{NH}_4\text{PO}_2(\text{OMe})_2$ (Giarda *et al.*, 1973) were determined by single-crystal X-ray analysis. Literature on acid ammonium phosphate monoesters, especially on their structural characterization, is much rarer. The ammo-

nium hydrogen phosphate esters $\text{NH}_4\text{PO}_2(\text{OH})(\text{OR})$ [$R = \text{Me}$ (1), Et (2)], known for a number of years (Neels & Grunze, 1982; Cavalier, 1898; Pimmer & Burch, 1929), and $\text{NH}_4\text{PO}_2(\text{OH})(\text{OPr}^i)$ could only be obtained in microcrystalline form. The soapy-like consistency and the scaly shape of the microcrystals implied a layered-type structure for these compounds, the $[\text{PO}_2(\text{OH})(\text{OR})]$ units probably being connected by an extended hydrogen-bonding network. As it was not possible to grow single crystals of these compounds the structure analysis from X-ray powder diffraction data was undertaken.

2. Experimental

Acid ammonium salts of monoalkyl phosphoric acids were synthesized by the reaction of ammonium diacetyl phosphate $\text{NH}_4\text{PO}_2(\text{OAc})_2$ with the corresponding alcohol ROH [$R = \text{CH}_3$ (1), CH_3CH_2 (2), $(\text{CH}_3)_2\text{CH}$ (3)]. In the first step the diacetyl phosphate, which is reasonably soluble in alcohol, was transformed into the acid monoacetyl phosphate. The latter reacted further with the alcohol to give the ammonium hydrogen alkyl phosphate (Neels & Grunze, 1982). Diethyl ether was added to the respective solutions to complete the precipitation process.



For (1) the X-ray powder diffraction data were first collected on a finely ground sample (side-loaded in a flat sample holder) using a Rigaku computer-automated diffractometer. The X-ray source was a rotating anode operating at 50 kV and 180 mA with a copper target and graphite-monochromated radiation. Data were collected between 5 and 80° in 2θ with a step size of 0.01° and a counting time of 10 s per step. As the powder pattern showed a pronounced preferred orientation

effect (Fig. 1a), the compound was prepared for a second X-ray experiment using a suspension chamber (Davis, 1986). The Tubular Aerosol Suspension Chamber (TASC) operates on the principle of dispersion of finely ground sample particles into an aerosol through the action of spherical beads. The aerosol is carried up through a column and is captured by a glass fibre filter mounted in a cassette by the action of a circulating pressure/vacuum pump. If the particle size of the sample is kept below 10 μm diameter the particles are captured in a random orientation within the pores between the glass fibres. Compound (1), prepared in this manner, was remeasured under the same conditions as described below (Fig. 1b). The difference in the intensities in the resulting powder pattern is remarkable.

X-ray powder diffraction data for (2) and (3) were measured in transmission mode (0.5 mm rotating capillary) on a high-resolution laboratory powder diffractometer (Stoe STADIP) using Cu $K_{\alpha 1}$ radiation (1.5406 Å). The data were collected for (2) every 0.02°

in 2θ from 5 to 80° with a counting time of 360 s per step, and for (3) every 0.01° in the same range with a counting time of 42 s per step. No major preferred orientation problems were visible in either powder pattern.

The powder patterns were indexed by Ito methods based on the first 20 observed reflections (Visser, 1969). The best solutions corresponded to monoclinic unit cells in each case. The indexed reflections showed systematic absences of the type $h0l$, $l = 2n$, $00l$, $l = 2n$, $0k0$, $k = 2n$, for (1) and (2), which is consistent with the space group $P2_1/c$, while for (3) the systematic absences of hkl , $k + l = 2n$, $h0l$, h , $l = 2n$, $0kl$, $k + l = 2n$, $hk0$, $k = 2n$, $h00$, $h = 2n$, $0k0$, $k = 2n$, $00l$, $l = 2n$, correspond to the non-centrosymmetric space group An , also taking into account the number of formula units per unit cell ($Z = 4$). Crystallographic details are given in Table 1. Molecular drawings were produced using the *PLUTON* software (Spek, 1990).

For (1) integrated intensities were extracted from the profile over the range $5 < 2\theta < 80^\circ$ by decomposition methods, as described by Rudolf & Clearfield (1989). This procedure produced 45 single indexed reflections up to a 2θ limit of 55°. A Patterson map was computed using this data set in the *TEXSAN* series of single crystal programs (Molecular Structure Corporation, 1989). The position of the P atom could be located from this Patterson map. The positions of the four O atoms bonded to P, one N and one C atom were obtained from difference-Fourier maps. This structural model was used for Rietveld profile refinement in *GSAS* (Larson & Von Dreele, 1994) using the profile over the range $5 < 2\theta < 80^\circ$. After the initial refinement of the scale, background and unit-cell constants, the atomic positions were refined using soft constraints consisting of P—O and C—C bond distances. The tetrahedral geometry around the P atom was fixed by the appropriate distances between the bonded O atoms. Final refinement was carried out with soft constraints for all the atoms. One impurity peak at $2\theta = 16.544^\circ$ corresponding to an unidentified phase was excluded from the calculations. The weight was reduced as the refinement progressed, but the constraints could not be removed completely without reducing the stability of the refinement. All atoms were refined isotropically. In the final cycles of refinement the shifts in all parameters were less than their e.s.d.'s. Neutral scattering factors were used for all atoms. No corrections were made for absorption effects or preferred orientation.

For (2) and (3) approximately 250 peaks were extracted using the program *EXTRA* (Altomare *et al.*, 1995). A Patterson map was computed using these data sets in the *SHELX* series of single-crystal solution programs (Sheldrick, 1990, 1993). The positions of the P atom and some O atoms could be located for each structure. The positions of the remaining atoms were located from difference-Fourier maps. Structures (2) and (3) were refined in *GSAS* (Larson & Von Dreele,

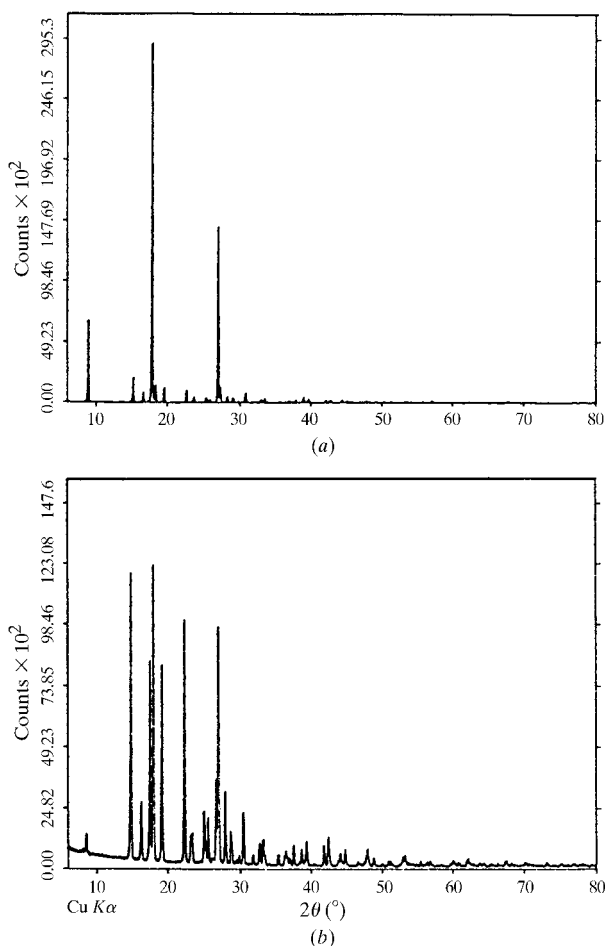


Fig. 1. Powder diffraction profile for (1): (a) the sample was side-loaded into a flat sample holder; (b) the sample was prepared using the TASC.

Table 1. *Experimental details*

	(1)	(2)	(3)
Crystal data			
Chemical formula	CH ₈ NO ₄ P	C ₂ H ₁₀ NO ₄ P	C ₃ H ₁₂ NO ₄ P
Chemical formula weight	129.04	143.10	157.13
Cell setting	Monoclinic	Monoclinic	Monoclinic
Space group	<i>P</i> 2 ₁ / <i>c</i>	<i>P</i> 2 ₁ / <i>c</i>	<i>An</i>
<i>a</i> (Å)	9.9645 (4)	12.6453 (4)	6.2475 (2)
<i>b</i> (Å)	7.1801 (3)	7.1502 (2)	29.3825 (6)
<i>c</i> (Å)	7.8897 (3)	7.9738 (2)	4.6305 (1)
β (°)	96.243 (3)	108.875 (2)	100.904 (2)
<i>V</i> (Å ³)	561.13 (4)	682.18 (3)	834.66 (3)
<i>Z</i>	4	4	4
<i>D</i> _x (Mg m ⁻³)	1.527	1.400	1.245
Radiation type	Cu <i>K</i> α ₁ , Cu <i>K</i> α ₂	Cu <i>K</i> α ₁	Cu <i>K</i> α ₁
Wavelength (Å)	1.5406, 1.5444	1.5406	1.5406
θ range (°)	2.5–40	2.5–40	2.5–40
μ (mm ⁻¹)	3.65	3.06	2.51
Temperature (K)	293	293	293
Data collection			
ρ_{calc} (g cm ⁻³)	1.527	1.400	1.245
Step size (2 θ)	0.02	0.02	0.02
Step scan time (s)	10	360	42
Data collection mode	Reflection	Transmission	Transmission
No. of contributing reflections	682 (<i>K</i> _{α1} + <i>α</i> ₂)	410	256
No. of structural parameters	14	14	17
No. of profile parameters	6	6	6
Refinement			
<i>R</i> _{wp} [†]	0.144	0.094	0.085
<i>R</i> _p [‡]	0.106	0.066	0.061
<i>R</i> _F [§]	0.094	0.098	0.067

[†] $R_{wp} = [\sum w(I_o - I_c)^2 / \sum w I_o^2]^{1/2}$. [‡] $R_p = \sum |I_o - I_c| / \sum I_c$. [§] $R_F = (|F_o| - |F_c|) / (|F_o|)$.

1994) using the profiles over the range $6 < 2\theta < 80^\circ$ in an analogous manner to that described above for (1). In contrast to (1) a correction was made for the preferred orientation effect using the March–Dollase method (Dollase, 1986) in *GSAS* (Larson & Von Dreele, 1994). For (2) the diffraction vector is along the *a** axis, hence the refined parameter was the ratio (1.094) of the effect along this axis to that lying in the plane perpendicular to this axis. For (3) the diffraction vector is along the *b** axis, hence the refined parameter was the ratio (0.949) of the effect along this axis to that lying in the plane perpendicular to this axis. Final Rietveld plots for all three compounds are given in Fig. 2. Positional and displacement parameters are listed in Table 2, and bond distances and angles in Table 3. A list of important intermolecular distances in the three compounds is given in Table 4.†

3. Results and discussion

In all three compounds the hydrogen alkyl phosphate units are connected to each other by an extended

hydrogen-bonding network, involving the hydroxyl groups of the ester and the ammonium cations, resulting in the formation of a double-layer framework.

The two-dimensional hydrogen-bonding network for (1) is shown in Fig. 3(a). The [010] projections for structures (1) and (2) are shown in Figs. 3(b) and 4, while a [100] projection of (3) is given in Fig. 5. In (2) and (3) the hydrogen alkyl phosphate units are connected to each other in a similar way. The intermolecular O···O and O···N distances are listed in Table 4. The bond distances and angles within the hydrogen alkyl phosphate groups for the three compounds are compared in Table 3. The mean P–O terminal bonds are in the range 1.482 (9)–1.595 (5) Å ($P-O_{av} = 1.542$ Å) and are almost the same in all three compounds, while the P–O(alkyl) bond lengths (P1–O1) decrease from 1.655 (6) Å in the methyl-substituted compound (1) to 1.512 (5) Å in the isopropyl phosphate compound (3). The O1–C1 distances also decrease slightly from 1.523 (7) Å for (1) to 1.456 (7) Å for (3). Each of the terminal O atoms (O2, O3 and O4) of the phosphate group is involved in the hydrogen-bonding network. A short intermolecular contact is observed between O atoms O2···O4; 2.573 (8) Å in (1), 2.615 (13) Å in (2) and 2.494 (9) Å in (3). The shortness of these non-bonded O···O distances indicates that the H atom may be half-way between the

† The numbered intensity of each measured point on the profile has been deposited with the IUCr (Reference: SH0104). Copies may be obtained through The Managing Editor, International Union of Crystallography, 5 Abbey Square, Chester CH1 2HU, England.

O atoms or statistically distributed between them. Hence, chains containing only $\text{PO}_2(\text{OH})(\text{OR})-$ units are formed. It was not possible to locate the H atom owing to the lack of information available when using laboratory X-ray powder data. One of the O atoms,

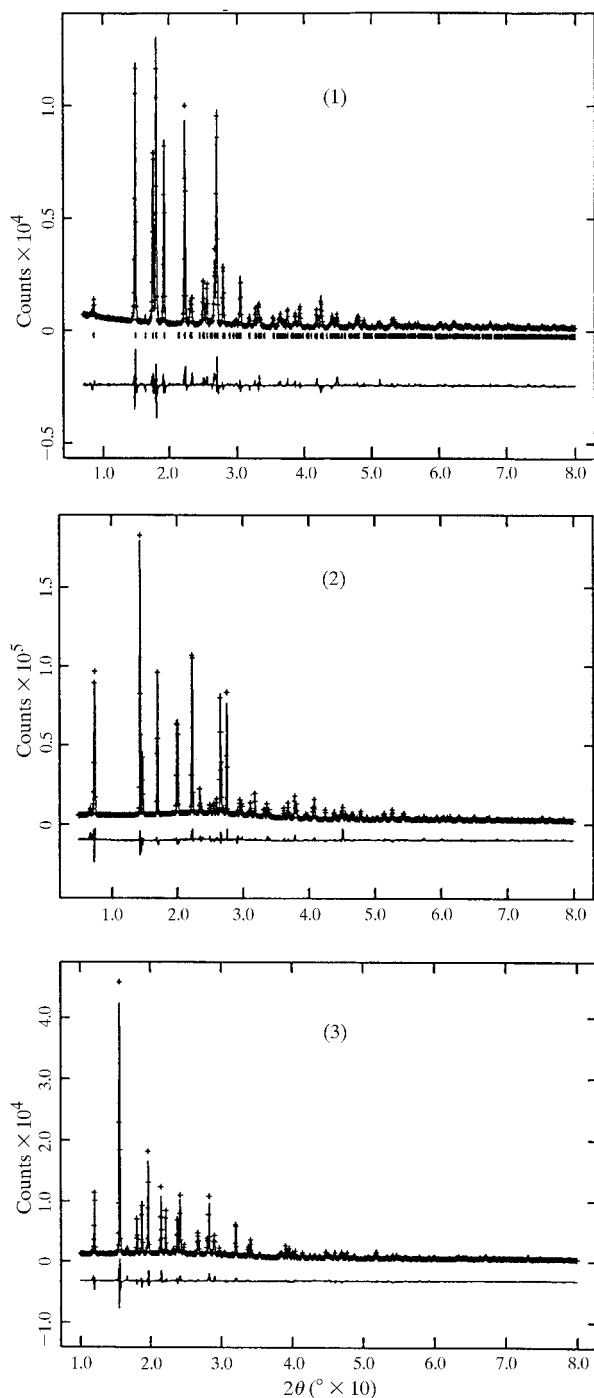


Fig. 2. Observed (+) and calculated (-) profiles for the Rietveld refinement of (1), (2) and (3). The bottom curve is the difference plot on the same intensity scale.

Table 2. Fractional atomic coordinates and equivalent isotropic displacement parameters (\AA^2)

$$U_{\text{eq}} = (1/3)\sum_i \sum_j U^{ij} a^i a^j \mathbf{a}_i \cdot \mathbf{a}_j.$$

	<i>x</i>	<i>y</i>	<i>z</i>	U_{eq}
(1)				
P1	0.2246 (4)	0.1052 (5)	0.2916 (5)	0.029 (4)
O1	0.3684 (6)	0.2176 (8)	0.2809 (9)	0.042 (6)
O2	0.1691 (6)	0.0280 (8)	0.1079 (7)	0.040 (5)
O3	0.2585 (6)	-0.0660 (8)	0.4024 (8)	0.043 (6)
O4	0.1270 (6)	0.2371 (9)	0.3615 (8)	0.029 (6)
C1	0.4743 (8)	0.110 (2)	0.195 (1)	0.046 (7)
N1	0.1643 (8)	0.6203 (9)	0.2270 (9)	0.008 (5)
(2)				
P1	0.1786 (5)	0.1037 (7)	0.3265 (7)	0.019 (3)
O1	0.2873 (9)	0.223 (1)	0.428 (2)	0.024 (2)
O2	0.1238 (7)	0.039 (1)	0.465 (1)	0.024 (2)
O3	0.2093 (8)	-0.072 (1)	0.246 (1)	0.024 (2)
O4	0.0992 (8)	0.238 (1)	0.209 (1)	0.024 (2)
C1	0.385 (1)	0.135 (2)	0.571 (2)	0.024 (2)
C2	0.473 (1)	0.298 (2)	0.633 (2)	0.024 (2)
N1	0.1311 (9)	0.608 (2)	0.377 (2)	0.024 (2)
(3)				
P1	0.5620 (7)	0.3322 (2)	0.410 (1)	0.038 (4)
O1	0.524 (1)	0.3804 (2)	0.503 (1)	0.024 (1)
O2	0.739 (1)	0.3349 (3)	0.203 (1)	0.024 (1)
O3	0.350 (1)	0.3080 (2)	0.239 (2)	0.024 (1)
O4	0.665 (1)	0.3059 (2)	0.687 (1)	0.024 (1)
C1	0.414 (1)	0.4163 (3)	0.315 (3)	0.024 (1)
C2	0.180 (1)	0.4218 (3)	0.351 (3)	0.024 (1)
C3	0.553 (1)	0.4573 (3)	0.314 (3)	0.024 (1)
N1	0.132 (2)	0.2850 (2)	0.717 (2)	0.024 (1)

Table 3. Bond distances (\AA) and angles ($^\circ$) for (1), (2) and (3)

	$\text{NH}_4\text{PO}_2(\text{OH})$ (OMe) (1)	$\text{NH}_4\text{PO}_2(\text{OH})$ (OEt) (2)	$\text{NH}_4\text{PO}_2(\text{OH})$ (OPr ⁱ) (3)
P1—O1	1.655 (6)	1.599 (9)	1.512 (5)
P1—O2	1.594 (5)	1.551 (9)	1.595 (5)
P1—O3	1.525 (5)	1.518 (9)	1.578 (6)
P1—O4	1.505 (5)	1.482 (9)	1.534 (6)
O1—C1	1.523 (7)	1.517 (14)	1.456 (7)
C1—C2		1.579 (14)	1.513 (8)
C1—C3			1.484 (7)
O1—P1—O2	109.9 (4)	107.9 (7)	106.7 (4)
O1—P1—O3	106.5 (4)	111.2 (7)	113.9 (8)
O1—P1—O4	108.1 (5)	105.8 (7)	107.1 (5)
O2—P1—O3	105.9 (4)	106.5 (6)	109.4 (4)
O2—P1—O4	112.2 (4)	106.1 (7)	107.4 (4)
O3—P1—O4	114.1 (5)	118.8 (6)	111.9 (4)
P1—O1—C1	114.8 (5)	121.0 (9)	126.1 (6)
O1—C1—C2		104.5 (11)	111.7 (7)
O1—C1—C3			112.3 (7)
C2—C1—C3			119.4 (7)

which participates in the $\text{O}\cdots\text{O}$ interaction (O4), forms two additional hydrogen bonds to symmetry-related ammonium counterions. The third terminal O atom (O3) is also linked to two symmetry-related ammonium counterions. As the ammonium ions provide a tetrahedral coordination sphere involving four O atoms, the hydrogen alkyl phosphate units are connected and thus

form double layers. The alkyl groups point away from the neutral double layers into the inter-layer space, thus connecting each other by van der Waals interactions. The shortest intermolecular distance, 3.443 (20) Å, was found in (2). The inter-layer spacing increases with the length of the alkyl group ($R = \text{Me}$: 9.96 Å, $R = \text{Et}$: 12.64 Å, $R = \text{Pr}^i$: 14.69 Å).

4. Conclusions

The phosphate ester P—O(alkyl) bond lengths in the methyl (1) and ethyl ester (2), 1.655 (6) and 1.599 (9) Å,

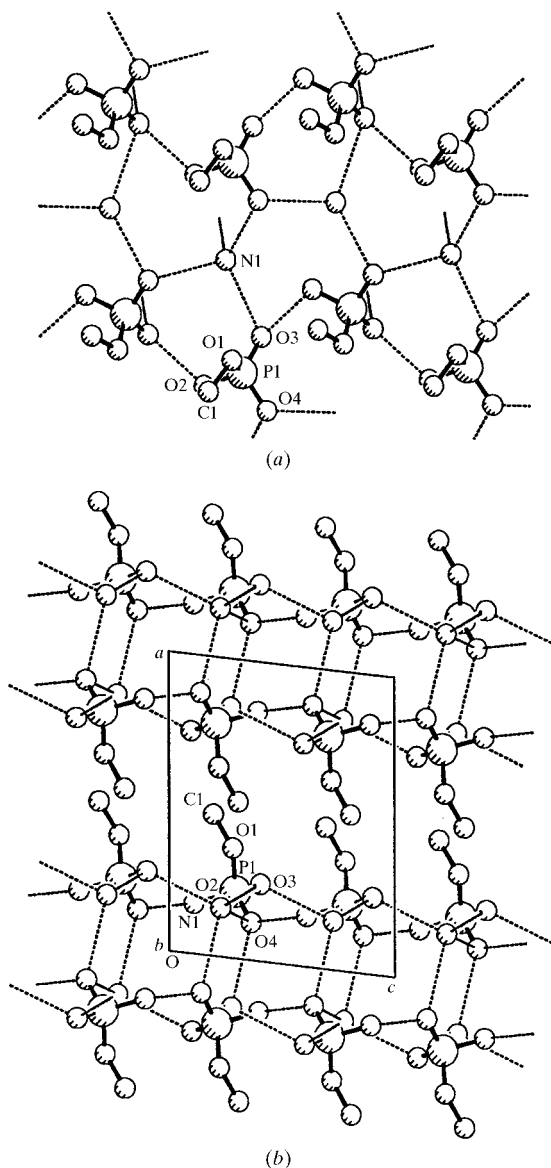


Fig. 3. Projection of the crystal structure of (1) along the (a) a and (b) b axes. The intermolecular contacts are indicated by dashed lines.

respectively, are significantly longer than the other three terminal P—O bonds ($P-O_{av} = 1.542$ Å). Compared with the analogous distances in other phosphate monoesters (Table 5), the distances are slightly longer in (1) and (2). Interestingly, the P—O(alkyl) bond in the isopropyl phosphate compound (3) [1.512 (5) Å] is shorter than the average P—O bond, probably as a result of the decrease in the P—O(alkyl) bond distance from the methyl to the isopropyl derivative. At the same time the P—O—C angle increases from 114.8 (5)° in (1) to 121.0 (9)° in (2) and to 126.1 (6)° in (3). The three terminal O atoms are involved in an extensive hydrogen-bonding network. Two O atoms are directly linked *via* the interaction between the H atom of the O—H group and the unprotonated O atom. The remaining two terminal O atoms function as acceptors for hydrogen bonds from the ammonium ions. Since the ester O atoms in (1)–(3) are less basic than the other three O atoms, they do not accept hydrogen bonds. The ammonium ions show a tetrahedral coordination, forming four hydrogen bonds to terminal O atoms of the ester phosphate groups.

In this type of compound the existence of hydrophobic and hydrophilic parts in the molecules has been shown previously to result in the formation of ribbon-like structures (Kerr *et al.*, 1979), channel compounds (Garbassi *et al.*, 1972) and layered structures (Giarda *et al.*, 1973). As shown in Figs. 3, 4 and 5, all three struc-

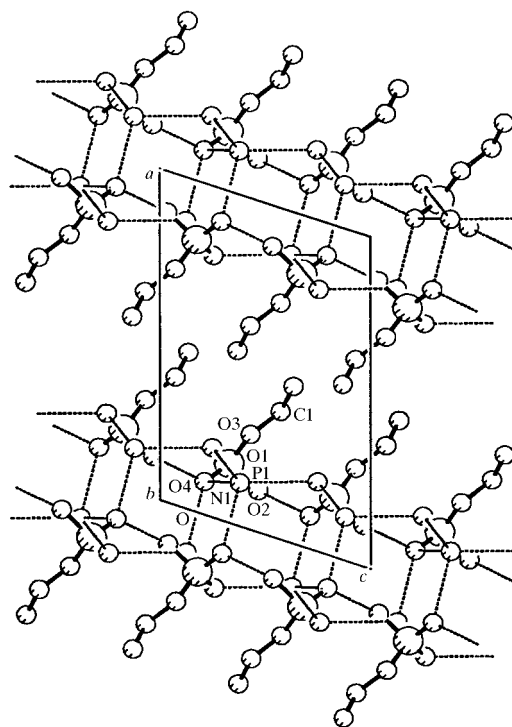


Fig. 4. The structure of (2) viewed down the b axis. Dashed lines indicate the intermolecular contacts.

Table 4. Intermolecular contacts in (1), (2) and (3)

Compound	Atoms	Distances (Å)	Atoms	Distances (Å)
NH ₄ PO ₂ (OH)(OMe) (1)	O2—O4 ⁱ	2.573 (8)	N1—O3 ⁱⁱ	2.754 (8)
			N1—O3 ⁱ	2.848 (8)
			N1—O4	2.987 (9)
			N1—O4 ⁱⁱⁱ	3.029 (9)
NH ₄ PO ₂ (OH)(OEt) (2)	O2—O4 ^{iv}	2.615 (13)	N1—O3 ⁱⁱ	2.820 (14)
			N1—O3 ^{iv}	2.800 (13)
			N1—O4	2.937 (14)
			N1—O4 ⁱⁱⁱ	2.918 (13)
NH ₄ PO ₂ (OH)(OPr ^t) (3)	O2—O4 ^v	2.494 (9)	N1—O3 ^{vi}	2.628 (10)
			N1—O3	2.893 (10)
			N1—O4 ^{vii}	2.955 (13)
			N1—O4 ^{viii}	2.685 (10)

Symmetry codes: (i) $x, \frac{1}{2} - y, -\frac{1}{2} + z$; (ii) $x, 1 + y, z$; (iii) $-x, \frac{1}{2} + y, \frac{1}{2} - z$; (iv) $x, \frac{1}{2} - y, \frac{1}{2} + z$; (v) $x, y, -1 + z$; (vi) $x, y, 1 + z$; (vii) $-1 + x, y, z$; (viii) $\frac{1}{2} + x, \frac{1}{2} - y, z$.

tures consist of double layers extending parallel to the *bc* plane in (1) and (2), and parallel to the *ac* plane in (3). The layers are separated from each other by van der Waals contacts between the hydrophobic alkyl groups. It can be seen that the larger the alkyl moiety, the larger

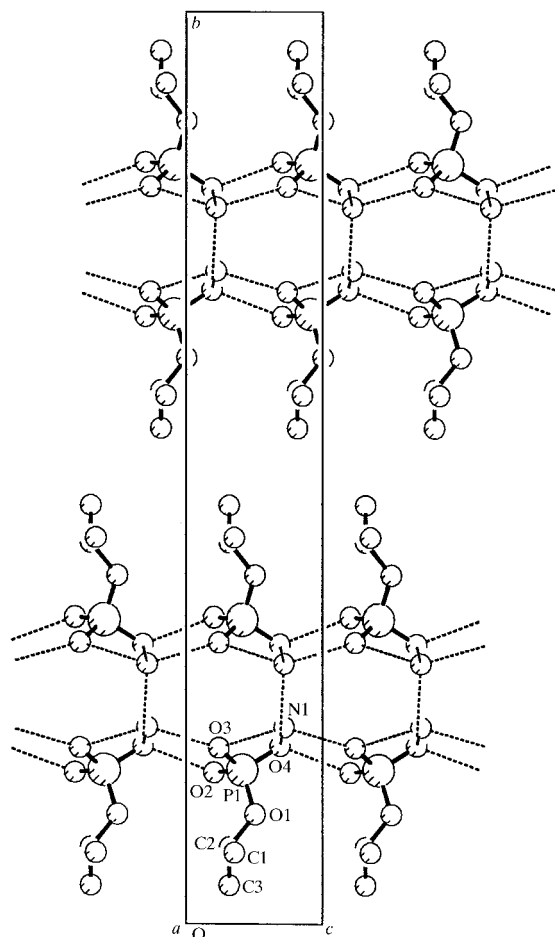


Fig. 5. A view of the structure of (3) down the *a* axis. The intermolecular contacts are shown by dashed lines.

Table 5. *P—O(C)* bond lengths (Å) in some phosphate monoesters

NH ₄ PO ₂ (OH)(OMe)	1.655 (6)	This work
(NH ₄) ₂ PO ₃ (OMe)·2H ₂ O	1.597 (6)	Garbassi <i>et al.</i> (1972)
Na ₂ PO ₃ (OMe)·6H ₂ O	1.626 (3)	Klooster & Craven (1992)
NH ₄ PO ₂ (OH)(OEt)	1.599 (9)	This work
K ₂ PO ₃ (OEt)·4H ₂ O	1.564	McDonald & Cruickshank (1971)
(C ₆ H ₁₄ N)PO ₃ (OEt)	1.579 (5)	Kerr <i>et al.</i> (1979)
NH ₄ PO ₂ (OH)(OPr ^t)	1.512 (5)	This work

the interlayer spacing, which effectively increases from 9.96 Å in (1) to 14.69 Å in (3).

The authors would like to thank the Laboratorium für Kristallographie of the ETH Zürich, in particular, the group of Professor Christian Baerlocher, and Stoe & Cie GmbH, Darmstadt, Germany, for enabling the diffraction experiments on (2) and (3) to be carried out. We also wish to thank the Swiss National Science Foundation for financial support and especially for a research grant for AN.

References

- Altomare, A., Burla, M. C., Cascarano, G., Giacovazzo, C., Guagliardi, A., Moliterni, A. G. G. & Polidori, G. (1995). *J. Appl. Cryst.* **28**, 842–846.
- Cavalier, J. (1898). *Bull. Soc. Chim. Fr.* **3**, 958–960.
- Davis, B. L. (1986). *Powder Diffr.* **1**, 240–243.
- Dollase, W. A. (1986). *J. Appl. Cryst.* **19**, 267–272.
- Garbassi, F., Giarda, L. & Fagherazzi, G. (1972). *Acta Cryst.* **B28**, 1665–1670.
- Giarda, L., Garbassi, F. & Calcaterra, M. (1973). *Acta Cryst.* **B29**, 1826–1829.
- Kerr, K. A., Fawcett, J. K., Coppola, J. C., Watson, D. G. & Kennard, O. (1979). *Acta Cryst.* **B35**, 2749–2751.
- Klooster, W. T. & Craven, B. M. (1992). *Acta Cryst.* **C48**, 19–22.

- Larson, A. & Von Dreele, R. B. (1994). *GSAS. Generalized Structure Analysis System*. Los Alamos National Laboratory, New Mexico, USA.
- McDonald, W. S. & Cruickshank, D. W. J. (1971). *Acta Cryst.* **B27**, 1315–1319.
- Molecular Structure Corporation (1989). *TEXSAN. Single Crystal Structure Analysis Software*. MSC, 3200 Research Forest Drive, The Woodlands, TX 77381, USA.
- Neels, J. & Grunze, H. (1982). *Z. Anorg. Allg. Chem.* **495**, 65–72.
- Pimmer, R. H. A. & Burch, W. J. N. (1929). *J. Chem. Soc.* pp. 292–300.
- Rudolf, P. R. & Clearfield, A. (1989). *Inorg. Chem.* **28**, 1706–1710.
- Sheldrick, G. M. (1990). *Acta Cryst.* **A46**, 467–473.
- Sheldrick, G. M. (1993). *SHELXL93. Program for the Refinement of Crystal Structures*. University of Göttingen, Germany.
- Spek, A. L. (1990). *Acta Cryst.* **A46**, C34.
- Visser, J. W. (1969). *J. Appl. Cryst.* **2**, 89–95.